Spatial-temporal potential exposure risk analytics and urban sustainability impacts related to COVID-19 mitigation: A perspective from car mobility behaviour

Jiang, Peng; Fu, Xiuju; Fan, Yee Van; Klemeš, Jiří Jaromír; Chen, Piao; Ma, Stefan; Zhang, Wanbing

DOI
10.1016/j.jclepro.2020.123673

Publication date
2021

Document Version
Final published version

Published in
Journal of Cleaner Production

Citation (APA)
Jiang, P., Fu, X., Fan, Y. V., Klemeš, J. J., Chen, P., Ma, S., & Zhang, W. (2021). Spatial-temporal potential exposure risk analytics and urban sustainability impacts related to COVID-19 mitigation: A perspective from car mobility behaviour. *Journal of Cleaner Production*, *279*, Article 123673. https://doi.org/10.1016/j.jclepro.2020.123673

Journal of Cleaner Production 279 (2021) 123673

Contents lists available at ScienceDirect

Journal of Cleaner Production

journal homepage: www.elsevier.com/locate/jclepro

Spatial-temporal potential exposure risk analytics and urban sustainability impacts related to COVID-19 mitigation: A perspective from car mobility behaviour

Peng Jiang [a, *], Xiuju Fu [a, **], Yee Van Fan [b], Jiří Jaromír Klemeš [b], Piao Chen [c], Stefan Ma [d], Wanbing Zhang [a]

[a] Department of Systems Science, Institute of High Performance Computing, A*STAR, Singapore, 138632, Singapore
[b] Sustainable Process Integration Laboratory – SPIL, NETME Centre, Faculty of Mechanical Engineering, Brno University of Technology - VUT Brno, Technická 2896/2, 616 69, Brno, Czech Republic
[c] Delft Institute of Applied Mathematics, Delft University of Technology, Delft, Netherlands
[d] Epidemiology & Disease Control Division, Ministry of Health, Singapore

ARTICLE INFO

Article history:
Received 21 May 2020
Received in revised form
10 July 2020
Accepted 8 August 2020
Available online 19 August 2020

Handling editor: Yutao Wang

Keywords:
Spatial-temporal analysis
Risk mitigation
COVID-19
Car mobility behaviour
Air-emission reduction
Flexible lockdown strategy

ABSTRACT

Coronavirus disease-2019 (COVID-19) poses a significant threat to the population and urban sustainability worldwide. The surge mitigation is complicated and associates many factors, including the pandemic status, policy, socioeconomics and resident behaviours. Modelling and analytics with spatial-temporal big urban data are required to assist the mitigation of the pandemic. This study proposes a novel perspective to analyse the spatial-temporal potential exposure risk of residents by capturing human behaviours based on spatial-temporal car park availability data. Near real-time data from 1,904 residential car parks in Singapore, a classical megacity, are collected to analyse car mobility and its spatial-temporal heat map. The implementation of the circuit breaker, a COVID-19 measure, in Singapore has reduced the mobility and heat (daily frequency of mobility) significantly at about 30.0%. It contributes to a 44.3%–55.4% reduction in the transportation-related air emissions under two scenarios of travelling distance reductions. Urban sustainability impacts in both environment and economy are discussed. The spatial-temporal potential exposure risk mapping with space-time interactions is further investigated via an extended Bayesian spatial-temporal regression model. The maximal reduction rate of the defined potential exposure risk lowers to 37.6% by comparison with its peak value. The big data analytics of changes in car mobility behaviour and the resultant potential exposure risks can provide insights to assist in (a) designing a flexible circuit breaker exit strategy, (b) precise management via identifying and tracing hotspots on the mobility heat map, and (c) making timely decisions by fitting curves dynamically in different phases of COVID-19 mitigation. The proposed method has the potential to be used by decision-makers worldwide with available data to make flexible regulations and planning.

1. Introduction

The outbreak of coronavirus disease-2019 (COVID-19) prompts a series of social, economic and environmental issues. It is yet difficult to project the lasting impacts, such as on the environment system and the public health system, due to the uncertainty over the shape of economic recovery. By 20 May 2020, over 5 M of COVID-19 cases have been confirmed in 216 countries (WHO, 2020). COVID-19 might coexist with us for a long time. Even after apparent elimination, a resurgence could be possible as late as 2024 (Kissler et al., 2020). Current priority has been given on treatment, vaccine development, containment and mitigation strategies to reduce the mortality and infection rate. Flattening the curve (Ferguson et al., 2020) is among the most discussed concept to suppress the surge in COVID-19 cases to support the functionality of

* Corresponding author. 1 Fusionopolis Way, #15-16, Connexis North Tower, 138632, Singapore.
** Corresponding author. 1 Fusionopolis Way, #16-24, Connexis North Tower, 138632, Singapore.
E-mail addresses: jiang_peng@ihpc.a-star.edu.sg (P. Jiang), fuxj@ihpc.a-star.edu.sg (X. Fu).

https://doi.org/10.1016/j.jclepro.2020.123673
0959-6526/

the healthcare system. Timing (Anderson et al., 2020) and timing configuration (Zhang et al., 2012) are the critical determinants in minimising the potential impacts. It can be achieved by containment strategies such as testing on a massive scale, tracing and quarantine. When the disease outpaces containment, it has to rely on mitigation strategies (Walensky and de Rio, 2020), such as social distancing, closures, movement restriction via circuit breaker and lockdown. For the implementation of mitigation policies (e.g. circuit breaker), there are many subsequent socio-economic impacts needed to be evaluated. For example, whether is the time of a mitigation policy cautious and prescient? How is the urban sustainability, especially in terms of economic sustainability (economic trend, economic recovery, etc.) and environmental sustainability (air emissions, solid waste pollution, electricity consumption, etc.)? How do decision-makers plan for the subsequent mitigation after the disease situation is relatively stable? With the help of urban sustainability analyses, effective decision-making and planning are essential during this critical period to make sure that the usage of limited resources is optimised. The spatial-temporal identification of potential risk with COVID-19 infection (Jia et al., 2020) can support decision-making and planning to enhance the success of mitigation implementation.

The decision-making and planning based on spatial-temporal data analytics have been applied in different areas or domains. Zhao et al. (2020) explored the urban risk reduction strategy by spatial-temporal statistics to guide hazard mitigation planning. Luo et al. (2019) assessed tourist behaviour based on spatial-temporal information of the venue check-in to improve the management of gaming destinations. Sikder et al. (2019) estimated the building intensity using spatial statistics to make data-driven planning decision for urban development. Xu et al. (2019) implemented spatial-temporal economic analysis to design and plan centralised or decentralised modes in a resource-oriented system. Nesoff et al. (2019) evaluated the attributable risk of pedestrian injury according to the spatial analysis of alcohol outlet location. The other studies include assessing (a) global spatial risk of highly migratory shark for ocean management (Queiroz et al., 2019), (b) temporal waste-dumping behaviour for waste management planning (Jiang et al., 2020) and infected plastics dumping (Klemeš et al., 2020a), (c) pollution risk area for urban soil risk management (Wu et al., 2019), (d) coastal flood risk for resilience mechanism (Rumson et al., 2019), and (e) spatial-temporal characteristics of environmental impacts for the refinement of heavy metal pollution control (Huang et al., 2019).

The spatial-temporal data analytics for epidemic and pandemic disease is relatively limited, especially for the ongoing COVID-19 problems. Modelling and analytics (Wang et al., 2020) have supported COVID-19 mitigation positively, as also reported by Gibney (2020). A new model that predicts the epidemic course for effective control strategy is proposed by Giordano et al. (2020), considering eight stages of infection susceptible. The probability that newly introduced cases could trigger outbreaks in the other location/countries has been calculated by Kucharski et al. (2020), based on the cases reported in Wuhan. The understanding of the early transmission dynamics of COVID-19 is useful for infection control measures. However, as the estimation is based on the pattern and statistic methodology that happened in other countries, it might be not fully reflecting the situation of a specific place. A spatial-temporal risk source model was developed by Jia et al. (2020) based on the population flow tracking using mobile phone data-based counts in China. The consideration of other possible influence factors with higher data availability could offer a more representative estimation. For example, Okunlola and Oyeyemi (2019) evaluated the risk of malaria transmission in Nigeria by environmental predictors based on the spatial-temporal analysis. Van Bavel et al. (2020) highlighted the role of social and behavioural science to support the COVID-19 pandemic response. The method proposed in this study envisages the potential exposure risk of COVID-19 based on a set of quantitative big urban data on car mobility behaviour before and during the circuit breaker (GOS, 2020).

Under the lockdown or circuit breaker situations, the mobility of the population worldwide presents a decreasing trend (Ghosh, 2020), which does a favour to reduce the potential exposure risk of COVID-19 in the crowds. This is the original intention of implementing the lockdown or circuit breaker policy. The mobility indices of driving, walking and transit have presented similar patterns (Apple, 2020). Such mobility patterns of six countries from different continents are shown in Fig. S1. Compared to the walking mobility data, the driving mobility data are much more easily accessible since residential car parks record and save high-resolution access information. In addition, the driving mobility near the residence has a better representative of the mobility of the residents during a circuit breaker compared to transit mobility, let alone that the disease pandemic in most countries drove population from municipal mass transport to cars. Biljecki (2020) suggested that car mobility information recorded by residential car parks can be a practical measure for the movement of people.

This study aims to analyse spatial-temporal potential exposure risks and urban sustainability impacts related to the circuit breaker measure in facilitating the containment and mitigation planning of COVID-19. Big urban data in Singapore are analysed to demonstrate the applicability of the proposed method in this study. Some researchers worried about a possible second coronavirus wave (Cyranoski, 2020). Singapore had been one of the countries threatened for a second wave by COVID-19. In March 2020, its effective control strategies were praised by WHO's experts. But the second attack of COVID-19 in April 2020 has been much more challenging to address. From the early morning of 07 April, Singapore implemented a soft circuit breaker policy (GOS, 2020). Under this policy, people were suggested staying at home but still permitted going outside for essential activities by keeping social distancing. Such moderate policy regulation has also been implemented in the USA, the UK and Spain (Cyranoski, 2020). This study investigates spatial-temporal big urban data analytics for intelligent decision support of flexible regulations and planning. The proposed method can assist in mitigating the current or future pandemic that has been suggested as one of the biggest threats in the new era. The novelties of this study are highlighted as follows:

i. Spatial-temporal car park availability data with high resolution are innovatively utilised for representing potential exposure risks related to COVID-19 to investigate the mitigation effect based on an extended Bayesian spatial-temporal model.
ii. The lag effect through the phase-related dynamic curve fitting is innovatively identified, which reveals the complex relationship between cumulative mobility and cumulative confirmed cases of COVID-19.
iii. Urban sustainability impacts in both environment and economy related to COVID-19 mitigation are examined and discussed based on the transportation-related air emissions, electricity consumption, waste generation statistics and economic statistics.

2. Material and methods

2.1. Data

Open-source data are used in this study. The residential car park information (e.g. name, address, and location with X and Y coordinates) in Singapore is available from the public data platform (GTA, 2020a). On the data platform, the data of car park availability (GTA, 2020b) of 1,904 residential car parks (Fig. 1) are updated at a minute level. More than 3 M pieces of data records (e.g. name, time of records, total lots and available lots as in Fig. 1) are saved every day. The 1,904 car parks are located in 31 regions among the 55 planned regions (DOS, 2019). The resident population in the 31 regions covers 99.3% of Singapore (DOS, 2019). The data platform provides an API documentation for data acquisition. For this dataset, it has been excluded the occasional outliers with total lots fewer than available lots. The data of mobility trend reports are from the Apple COVID-19 data platform (Apple, 2020). The data on transportation fuel (CSD, 2020) and data on half-hourly electricity system demand (EMA, 2020) are used to estimate the environmental impacts of the circuit breaker. The data on the daily number of infected COVID-19 cases are from the COVID-19 Interactive Situation Report of Ministry of Health (MOH) in Singapore (MOH, 2020).

Despite a comparatively tiny area of 719.1 km^2, Singapore has close to 1 M vehicle population (Diao, 2019). Like the data platform on car park availability, other data platforms also provide relevant data. For example, the Singapore Traffic Watch project (SGTrafficWatch, 2020) offers nation-level and region-level traffic conditions, especially the hourly bus observation counts and the available taxis for hire in the last 24 h. Since the main objective of this study is to measure spatial-temporal potential exposure risks through near real-time car mobility changes before and during the circuit breaker, attention is primarily focused on the data coverage in space and time and the data accessibility. This motivates us to highlight the high-resolution data on nationwide car park availability up to several months. After checking for public data online in Singapore, this data set is undoubtedly the most suitable one to achieve the research objective.

2.2. Method

2.2.1. Definition of mobility, heat and exposure

Several terms used in this study are defined as follows:

Mobility: The times of cars moving in and out car parks. The cars include private cars and service cars, such as taxis, Uber cars and Grab cars.

Heat (the daily frequency of mobility): A relative concept by comparing total daily mobility with the corresponding total number of car park lots represented in the heat maps. The heat maps are referred to as pictures or maps that use colours to show different levels of activity frequency or values of something in different places.

Exposure: Civic activities exposing to the active population who are not staying at home and may carry coronavirus. A similar concept can be found as 'community exposure' and 'potential exposure' in NCIRD (2020) and 'exposure risk' in He et al. (2020).

Potential exposure risk is defined as the potential risk caused by exposing to the active population during disease pandemic. The exposure may cause potential 'exposure risk' (Lai et al., 2020) of coronavirus contact or disease infection. Since real data on the behaviour changes of mask-wearing and social distancing are unavailable, the actual exposure risk is challenging to measure. In this study, it has been assumed that a region with higher heat offers higher potential exposure risk for civic activities. The exposure risks in space or time mentioned in the following text are all under such a definition.

Expressions of daily mobility and heat at a different spatial scale are given as follows:

Car park-level mobility $m_{i,k}$ in Eq. (1) is denoted as the cumulative daily number of total changes in car park available lots:

$$m_{i,k} = \sum_{t} C_{i,k,t}, \ \forall i, \ \forall k, \tag{1}$$

where i is the index of residential car parks; k is the index of days; t is the index of minutes (00:00 to 24:00) in a day; $C_{i,k,t}$ denotes the minutely cumulative counts of the changes of car park available lots associating to the car park i on day k.

Region-level mobility $M_{j,k}$ in Eq. (2) equals the summation of the car park-level mobility on a regional scale:

$$M_{j,k} = \sum_{i \in j} m_{i,k}, \ \forall j, \ \forall k, \tag{2}$$

where j is the index of different regions.

Nation-level mobility M_k in Eq. (3) equals the summation of region-level mobility:

$$M_k = \sum_{j} M_{j,k}, \ \forall k. \tag{3}$$

The definition of mobility can be extended to define the departing/arriving mobility by counting the cumulative increasing/decreasing number of 'available lots' separately.

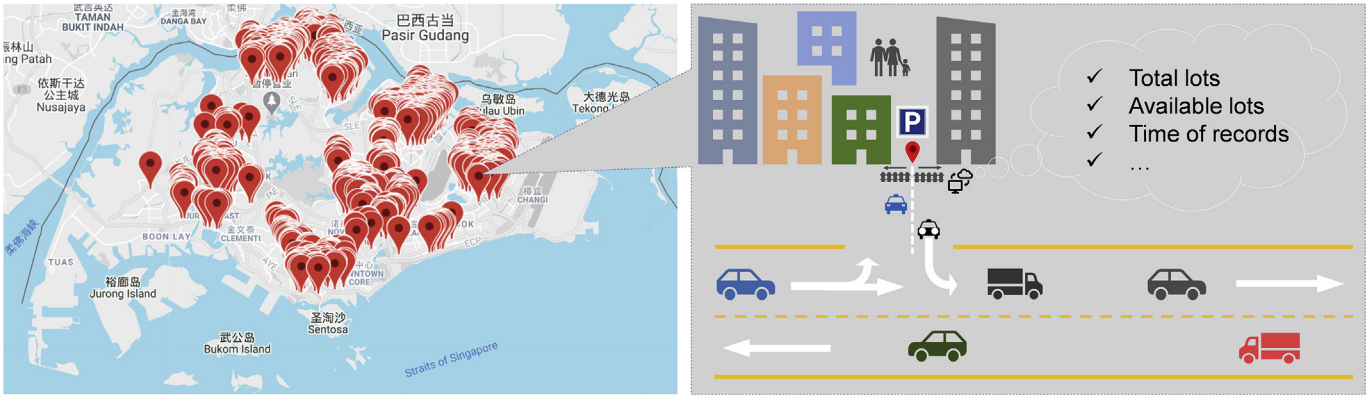

Fig. 1. The study sites (GTA, 2020a) and the diagram of one residential car park.

Car park-level heat $h_{i,k}$ in Eq. (4) is expressed as the division of the car park-level mobility to the number of total lots of a specific car park:

$$h_{i,k} = m_{i,k}/N_i, \forall i, \forall k, \tag{4}$$

whereN_i is the total car park lots of car park i. After multiple experiments, outliers of heat values have been observed most likely for those car parks with fewer than 30 total lots. Such car parks are filtered in this study.

Region-level heat $H_{j,k}$ in Eq. (5) is expressed as the division of the region-level mobility to the number of total lots of a specific region:

$$H_{j,k} = M_{j,k} \Big/ \sum_{i \in j} N_i, \forall j, \forall k \tag{5}$$

Although the region-level heat could be a robust heat measure by eliminating the interference from the extreme values related to individual car parks, the regions with very few car parks should be filtered for a fair comparison among different regions. This is further illustrated in Section 3.6.

2.2.2. Relationship analyses for cumulative mobility and cumulative cases

In Singapore, to figure out the source of infected cases, the COVID-19 cases are counted by four categories: imported cases from foreign countries (Source #1), community cases from Singapore residents and permanent residents (Source #2), cases from work permit holders who are not living in workers' dorms (Source #3) and cases from work permit holders who are living in workers' dorms (Source #4) (MOH, 2020). This study focuses on the "exposure-related cases", including cases in Source #2, cases in Source #3 and some early-time cases in Source #4 before the isolation of this source group. The imported cases and those cases of confined areas are out of the explanation scope of the defined exposure in this study.

Fig. 2 shows the crucial time points of regulation policies in Singapore from 15 March to 04 May 2020 (the studied time duration). The circuit breaker policy was implemented from the early morning of 07 April 2020. By this key time point, the studied time duration can be naturally divided into two parts to understand better the changes in the relationship between population mobility and infected cases. In contrast, the time series of COVID-19 cases is not separated directly by the beginning time of the circuit breaker, considering the potential incubation period (i.e. time to onset) of COVID-19 and the interval between onset and reporting dates. A five-day incubation period was reported based on the average results from the first 425 laboratory-confirmed patients in Wuhan (Li et al., 2020) and 181 worldwide confirmed cases outside Wuhan (Lauer et al., 2020). The median incubation period was reported as four days with a mean time to onset, 4.77 days, based on samples in Singapore (Pung et al., 2020). Both the incubation time and the interval between onset and reporting dates are uncertain for individual persons. In a macro view, the lag period between population mobility and infected cases should be treated as a variable rather than calculated by patient statistics and reporting dates directly. Such a variable can be optimally determined by curve fitting results. By assuming a six-day lag period as an example, the corresponding matching is shown in Fig. 2. Consequently, Phase I and Phase II can be divided accordingly. Since the incubation period has uncertainties (Li et al., 2020), cumulative values of mobility and cases, instead of daily values, are taken for relationship analyses. As shown in Fig. 2, the cumulative infected cases of Phase I match with cumulative mobility from 15 March to 06 April 2020 (i.e. before the circuit breaker). The cumulative cases of Phase II match with cumulative mobility from 07 April to 28 April 2020 (i.e. during the circuit breaker). The best curve fitting among the linear, polynomial, exponential, power and logarithmic functions is determined by the criterion of the smallest sum of squared residuals (SSR, also known as the residual sum of squares). For avoiding overfitting, the degree of the polynomial function is restricted to be less than or equal to 3.

2.2.3. Air emissions estimation based on mobility changes

The transportation-related average air emissions in Eqs. (6) and (7) are estimated according to the air emissions estimation framework in Fan et al. (2019). E_e^b in Eq. (6) and E_e^d in Eq. (7) denote the average air emissions before the circuit breaker (a total of K_1 days from 15 March to 06 April 2020) and during the circuit breaker (a total of K_2 days from 07 April to 28 April 2020). e is an index for a different type of emissions (i.e. CO_2, NO_x, SO_2 and PM). M_k is the nation-level daily mobility in Eq. (3). $M_k/2$ calculates the daily number of trips as M_k counts both daily departing and arriving activities. F_e is an emission factor (Table 1) of different type of pollutants/emissions. The emission factor applied in this study is based on the passenger transport report (CE Delft, 2020). The well to wheel (i.e. well to tank and tank to wheel in Table 1) life cycle (Fan et al., 2019) is considered. P is the average number of passengers. D^b and D^d represents the average distance travelled per trip before and during the circuit breaker. The assumptions of the calculation specifically for the case of Singapore include that (a) the main transportation fuel is petrol (CSD, 2020), (b) the car

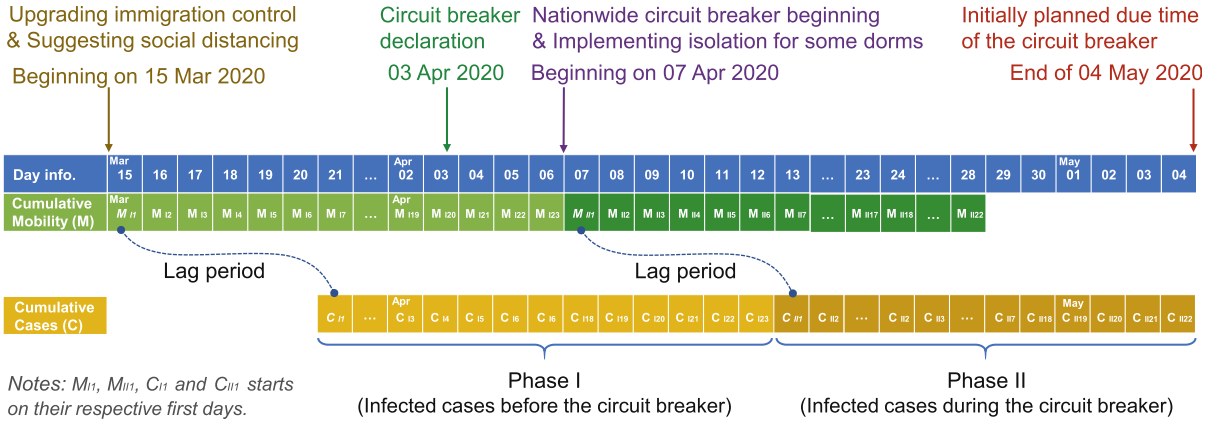

Fig. 2. Crucial time points of policies and two-phase division of the studied time duration.

Table 1
The type of emissions and the corresponding emission factors (CE Delft, 2020).

Type of Emissions	Well to Tank (g/pkm)	Tank to Wheel (g/pkm)	Emission Factor (g/pkm)
CO_2	28	134	162
NO_x	0.09	0.1	0.19
SO_2	0.244	0.0018	0.246
PM	0.01	0.003	0.013

occupancy rate is 1.7 passengers (DBS, 2020), (c) the average distance travelled using car before the circuit breaker is 18.59 km (Numbeo, 2020), and (d) 25.0% (Scenario 1) to 40.0% (Scenario 2) reduction in average distance travelled are considered during the circuit breaker (Unacast, 2020).

$$E_e^b = \frac{1}{K_1}\sum_{k=1}^{K_1}\frac{M_k}{2}F_e PD^b, \forall e, \tag{6}$$

$$E_e^d = \frac{1}{K_2}\sum_{k=K_1+1}^{K_1+K_2}\frac{M_k}{2}F_e PD^d, \forall e. \tag{7}$$

2.2.4. Modelling for spatial-temporal exposure risk mapping

Bayesian statistical models have advantages to take into account i) uncertainties in data, ii) missing data and iii) uncertainties in parameter estimation (Cressie and Wikle, 2015). For understanding the spatial-temporal relationship better and addressing uncertainties in individual days, an extended Bayesian spatial-temporal model with Poisson regression in Eqs. (8)–(11) based on the basic spatial-temporal model (Blangiardo and Cameletti, 2015) is built for the spatial-temporal potential exposure risk mapping:

$$Y_{jk} = \left[\alpha y_{jk}\right], \tag{8}$$

$$Y_{jk} \sim \text{Poisson}(\lambda_{ik}), \tag{9}$$

$$\lambda_{jk} = b_0 + u_j + v_j + \gamma_k + \varphi_k + \delta_{jk}, \tag{10}$$

$$\boldsymbol{R}_\delta = \begin{cases} \boldsymbol{R}_v \otimes \boldsymbol{R}_\varphi, if \quad Type\ I \\ \boldsymbol{R}_v \otimes \boldsymbol{R}_\gamma, if \quad Type\ II \\ \boldsymbol{R}_\varphi \otimes \boldsymbol{R}_u, if \quad Type\ III \\ \boldsymbol{R}_u \otimes \boldsymbol{R}_\gamma, if \quad Type\ IV \end{cases}, \tag{11}$$

where y_{jk} denotes heat in region j and day k, which is a continuous variable with a maximal value generally less than 10 for the regional-level car parks. Let Y_{jk} be a rounded value of αy_{jk} in region j and day k, where α, being an integer (order of magnitude, e.g. 10, 100 and 1,000), is a coefficient to ensure that Y_{jk} has enough identifiability for different regions. After experiments, it is valid to set α to be greater than or equal to 100. The α is set as 1,000 for the Singapore case. The scaled values $\{Y_{jk}\}$, counts of $[\alpha y_{jk}]$, are independently identically Poisson distributed with a distribution parameter λ_{jk}. The λ_{jk} is then modelled as a regression associating with spatial exposure risks and temporal exposure risks. The b_0 denotes the bias of the regression model. The overall risks $u_j + v_j + \gamma_k + \varphi_k + \delta_{jk}$ can be decomposed into the baseline temporal risks $\gamma_k + \varphi_k$, the intrinsic spatial risks $u_j + v_j$ and the spatial-temporal interacted risks δ_{jk}. The parameter vector $\boldsymbol{\delta}$ follows a Gaussian distribution with a precision matrix $\tau_\delta \boldsymbol{R}_\delta$, where τ_δ is a scalar constant and $\boldsymbol{R}_\delta$ in Eq. (11) is a structure matrix. $\boldsymbol{R}_u$, $\boldsymbol{R}_v$, $\boldsymbol{R}_\gamma$ and $\boldsymbol{R}_\varphi$ are also structure matrices. The notation $\otimes$ denotes the Kronecker product. Four interaction types (i.e. Types I, II, III and IV) were provided in Blangiardo and Cameletti (2015). The parameters of the regression model are estimated by a computationally effective algorithm, integrated nested Laplace approximations (INLA) (Rue et al., 2009) that has been proven to be an efficient alternative to the Markov Chain Monte Carlo (MCMC), on the R package R-INLA platform (Lindgren and Rue, 2015). As recommended by Zhang et al. (2019), the most commonly used deviance-based criterion of model selection for Bayesian models, the deviance information criterion (DIC) (Spiegelhalter et al., 2002), is employed to select the best one from different spatial-temporal interactions based on Types I to IV.

3. Results

3.1. Changes in car mobility behaviour

Fig. 3 shows the distributions of car mobility before and during the circuit breaker. Conventional patterns (Sun and Axhausen, 2016) are observed before the circuit breaker (Fig. 3a, 3b and 3c), where the morning, noon and evening peaks are apparent on working days. The total mobility is much larger than that during the circuit breaker (Fig. 3d, 3e and 3f). Car mobility in Fig. 3e decreases significantly. Compared to that on 06 April 2020, the reduction rate of the nation-level mobility elevates from 13.4% (07 April 2020) to 36.4% (12 April 2020) (Fig. S2). From 12 April to 28 April 2020, the reduction rate maintains at around 30.0% (Fig. S2). The calculated rates are in line with the results in the same period based on the mobility trends reports (Apple, 2020). During the circuit breaker, the morning peaks on working days almost disappear, which are dominated slightly by the noon peaks. More details about the departing and arriving car mobility are presented in Fig. S3. The results in Fig. 3 and Fig. S3 suggest that the circuit breaker measure in Singapore has been taken seriously. The changes in daily mobility are linked with the variation in the potential exposure risk of COVID-19.

3.2. The spatial-temporal trend of mobility

Fig. 4 shows the spatial-temporal trend of region-level mobility. The results cover around three-week before and three-week after the circuit breaker policy. Before 07 April 2020, the region-level mobility is relatively stable. Before the circuit breaker, spatial mobility on 03 April and 06 April 2020 are elevated compared to other days. This can be explained as the circuit breaker policy was declared at 4 p.m. on 03 April 2020. Mobility was therefore elevated on the last two working days (03 April and 06 April 2020). The region-level mobility changes significantly during the first week of the circuit breaker. Compared to that on 06 April 2020, mobility in nearly all regions in this week is reduced. This is in line with the reduction rate of nation-level mobility in Fig. S2. The spatial-temporal mobility is relatively stable in the following two weeks.

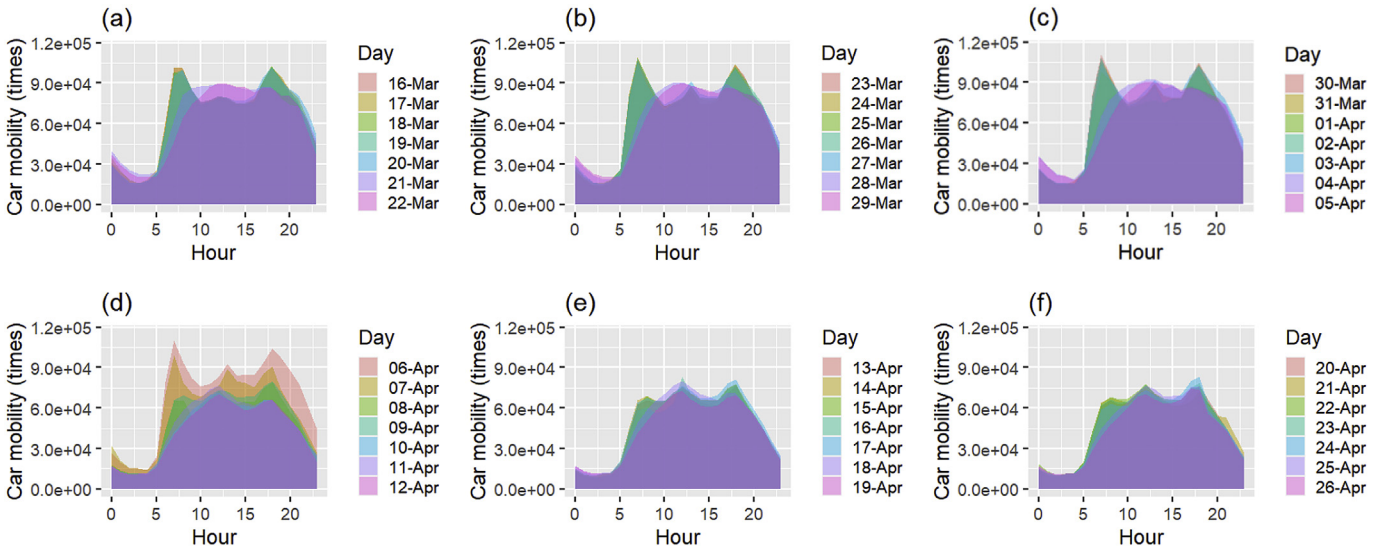

Fig. 3. Distributions of car mobility (a) 16 March (Monday) – 22 March (Sunday) 2020, (b) 23 March – 29 March 2020, (c) 30 March – 05 April 2020, (d) 06 April – 12 April 2020, (e) 13 April – 19 April 2020 and (f) 20 April – 26 April 2020.

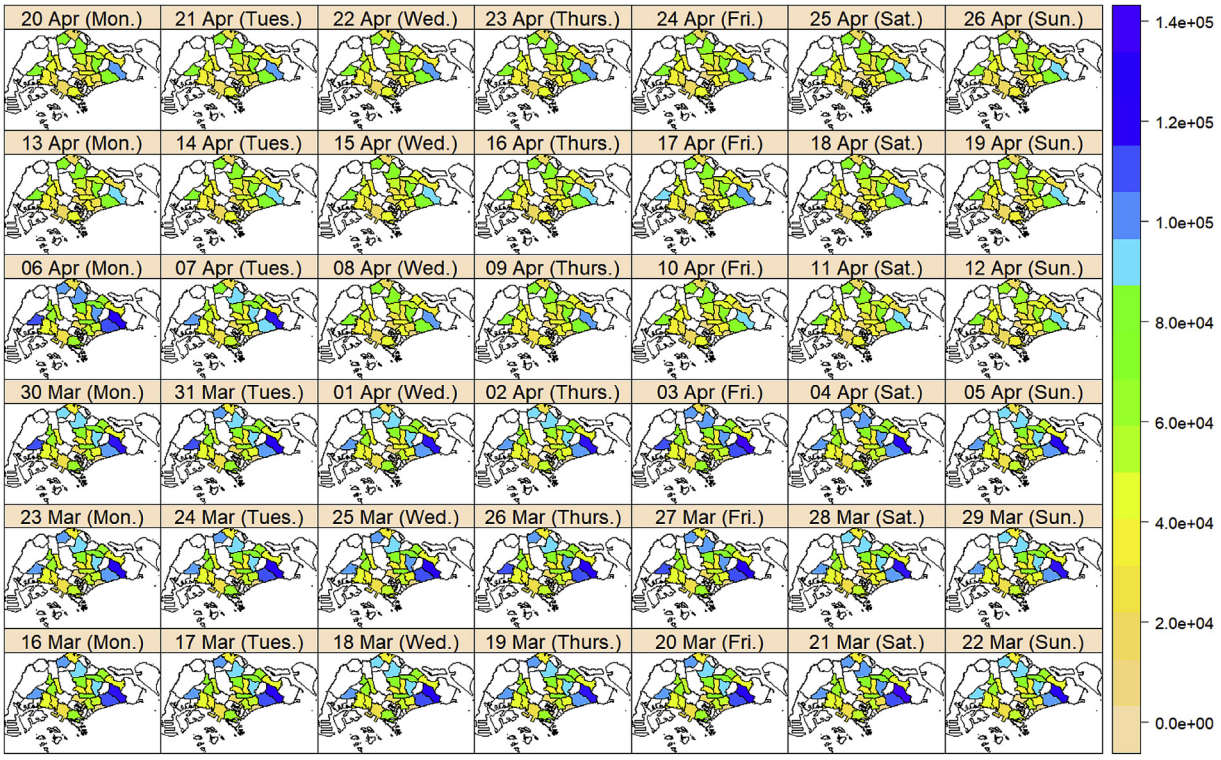

Fig. 4. The spatial-temporal trend of region-level mobility from 16 March (Monday) to 26 April (Sunday) 2020. Spatial mobility results related to 15 March and 27–28 April are omitted for ease of the weekly presentation. Regions with white colour are areas without residential car parks, including the central water catchment, western water catchment, western islands, north-eastern islands and southern islands. (For interpretation of the references to colour in this figure legend, the reader is referred to the Web version of this article.)

3.3. Curve fitting between cumulative mobility and cumulative cases

Fig. 5a shows the relationship between the cumulative lagged mobility and the cumulative cases (i.e. exposure-related confirmed cases) from 21 March to 04 May 2020 (Phases I & II). The variation is significant in the growth-trend of exposure-related cases before and after the dividing line in Fig. 5a. When data from two phases are merged, it is difficult to fit the curve via a smoothing function. By testing in the time duration before the circuit breaker, Table 2 compares the sum of squared residuals (SSR) under different lag periods of the cumulative mobility ranging from 0 to 7. The best-fitting result with the smallest SSR, i.e. 24,083, occurs when the lag period equals 6. The optimal six-day lag period (Table 2) and the beginning time of the circuit breaker (07 April 2020) are then utilised to determine the time duration of Phase I (from 21 March to 12

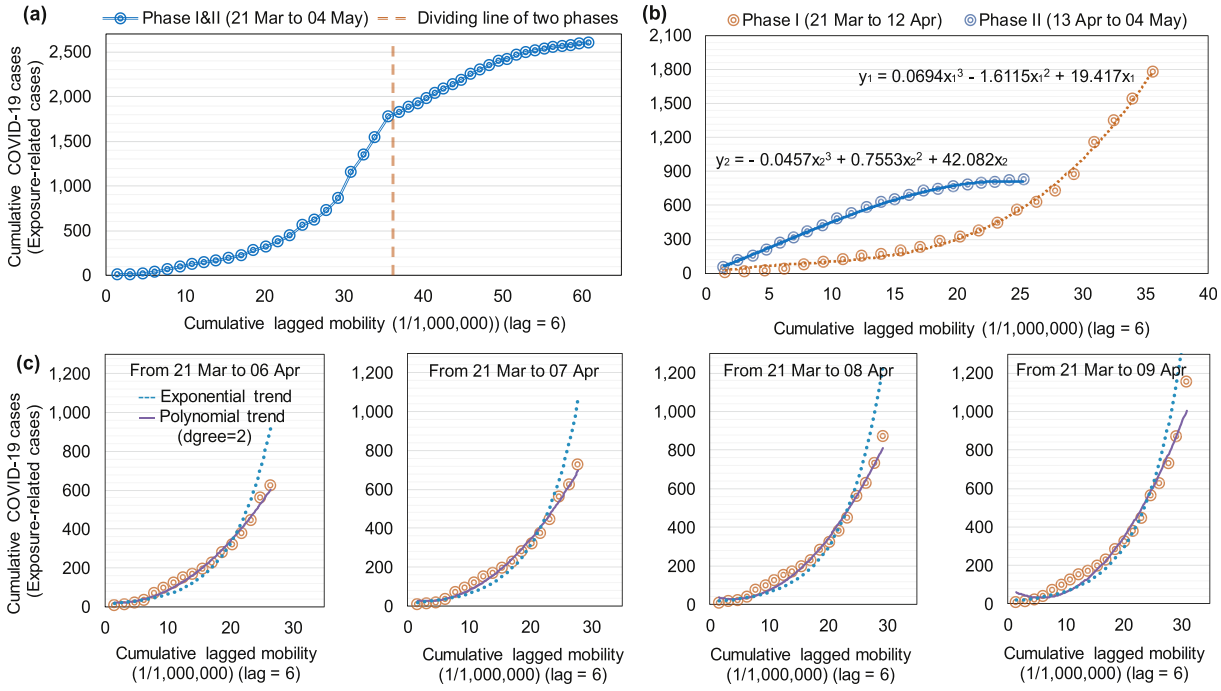

Fig. 5. The curve fitting between the cumulative lagged mobility and cumulative cases. (a) Data visualisation by merging two phases. (b) The phase-related curve fitting under a six-day lag by separating two phases. (c) Dynamic curve fitting results in Phase I.

Table 2
The comparison of curve fitting under different lag period settings.

Lag (d)	0	1	2	3	4	5	6	7
SSR	66,377	57,063	41,904	30,472	25,529	24,236	24,083	26,624

April 2020) and Phase II (from 13 April to 04 May 2020) in Fig. 5b. Three-order polynomial curves fit both phases well. The fitted curve in Phase I has a convex trend with a more and more steep slope near 12 April 2020. The fitted curve in Phase II has a concave trend with a more and more relaxed slope near 04 May 2020. The better phase recognition and phase division help to understand the disease outbreak trend and the policy effects. More discussion is provided in Section 4. The above evidence demonstrates the potential relationship between the cumulative lagged mobility and cumulative cases. Fig. 5c shows the dynamic curve fitting results for Phase I. The two-order polynomial trend fits the relationship well from 21 March to 06 April 2020. The fitting effect gets worse during the incubation period after starting the circuit breaker on 07 April 2020. In contrast, the exponential trend approaches the relationship better and better. For the curve fitting in Fig. 5, as the parameters of functions are time-varying with the increasing of cumulative cases, we do not intend to attract focus on the specific fitting functions. Instead, we aim to emphasise the benefit of phase recognition and the aid of emergent situation assessment via the dynamic curve fitting.

3.4. Air emissions changes based on the mobility

Fig. 6a and b show the comparison of the transportation-related average air emissions estimation before and during the circuit breaker. Compared the duration before the circuit breaker (15 March to 06 April 2020), the reduction rate of the transportation-related average air estimations during the circuit breaker (07 April to 28 April 2020) is calculated as 44.3% (Scenario 1) and 55.4% (Scenario 2). For example, the NO_x emissions are estimated to reduce from 4.65 kt to 2.59 kt (Scenario 1) or 2.07 kt (Scenario 2). The reduction is significant to the transportation sector in Singapore, as the cars and taxis are the major motor vehicle group (68.4%) of fuel consumption (CSD, 2020). The positive impact of the adopted measure due to the COVID-19 outbreak to the environment is also reported in Europe (Collivignarelli et al., 2020). However, the lasting impact on the environmental stimulates by the change in economic structure, and the policy is yet to be assessed as discussed by Klemeš et al. (2020b). A contradict opinion is also suggested by UNenvironmnet (2020) on the CO_2 emission. In addition to the transportation-related air emissions, the electricity and heating system also deserves an investigation. Based on the half-hourly electricity system demand data (EMA, 2020) from the Energy Market Authority in Singapore, the average daily electricity consumption during the circuit breaker is calculated as a 6.7% reduction compared to that before the circuit breaker. By weighting the effects in air estimations reductions from the transportation system and the electricity system in Singapore, the final percentage of emission reduction should be basically in line with the 30.0% reduction in Singapore reported by Fogarty (2020). Notably, the lasting reduction in emissions cannot be expected without a fundamental shift in global energy production and the reduction in deforestation and wildfires.

3.5. Spatial-temporal heat map of car mobility

Fig. 7a shows the average car mobility from 07 April to 28 April 2020 for a total of 1,904 residential car parks in Singapore. The mobility in the east-southern area is relatively higher than that in the north-western area. The mobility ranges from 0 to 2,736.82 with a mean of 680.49, a sample skewness of 0.99 and a variance of 185,410. Among a total of 17 distributions, the best-fitted distribution of mobility (Fig. 7b) obeys a Generalised Extreme Value (GEV) distribution with a shape parameter of 0.021, a scale parameter of 329.70 and a location parameter of 482.10 (Table S1).

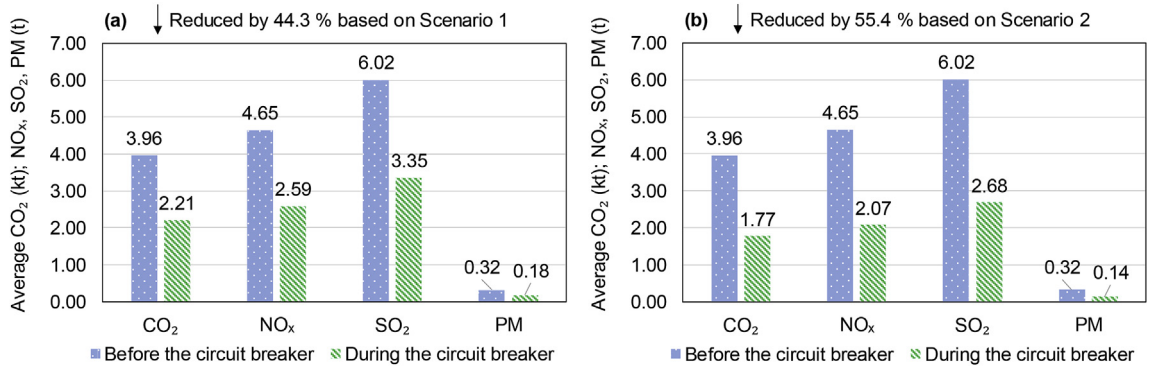

Fig. 6. The comparison of the transportation-related average air emissions estimation before and during the circuit breaker under (a) the 25.0% (Scenario 1) and (b) the 40.0% (Scenario 2) reduction in average distance travelled. For air emissions, four components are analysed, i.e. CO_2, NO_x, SO_2 and particulate matter (PM). The reported units for CO_2 is kt, NO_x, SO_2 and PM are t.

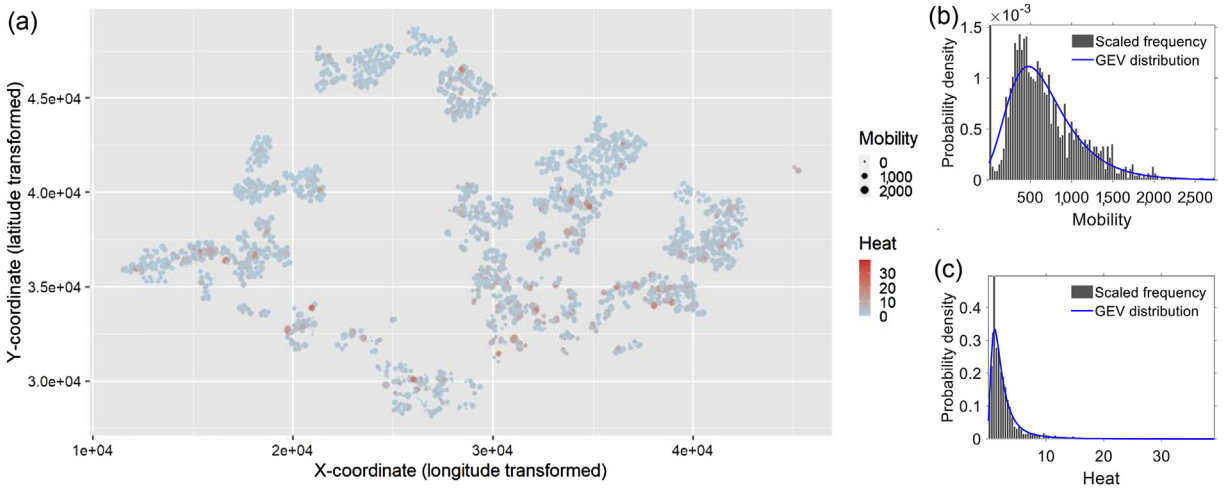

Fig. 7. (a) The residential car park locations in Singapore, the average car mobility from 07 April to 28 April 2020 and the corresponding spatial heat map. (b) The best-fitted probability distribution of mobility. (c) The best-fitted probability distribution of heat, where the histograms are transformed into scaled frequencies to display the probability distribution fitting and the histogram synchronously. The X and Y coordinates are in Geodetic CRS: SVY21 (GTA, 2020a).

By the spatial heat map in Fig. 7a, heat ranges from 0 to 39.15 with a mean of 2.81, a sample skewness of 3.86 and a variance of 11.31. The estimated parameters of the best-fitted GEV distribution of heat (Fig. 7c) are 0.39, 1.17 and 1.39 (Table S2). The probability distributions of mobility and heat have a similar longtail characteristic, although the longtail of heat is more intuitive than that of mobility. The intersection of both longtail parts corresponds to these hotspots in Fig. 7a, i.e. points with high mobility and high heat.

Among the 1,904 residential car parks, the first half car parks (i.e. 957) with higher average mobility from 07 April to 28 April 2020 are selected for the temporal heat map analyses. The temporal heat map of the top 50 most active ones (i.e. car parks with higher average heat values) among the 957 car parks is shown in Fig. 8. For each identified car park in the vertical axis of Fig. 8, its temporal heat values from 07 April to 28 April 2020 (i.e. the horizontal axis) are visualised with coloured rectangles. The darker red rectangle means higher heat. Judged by the heat range in the legend of Fig. 8, these car parks correspond to the longtail part in Fig. 7c. Among the 50 active car parks, C2, C3, C13, C18, C28, C29, C36 and C45 are suspected of not following the regulations strictly during the circuit breaker. In addition, the temporal heat map suggests that the mobility on 16 April 2020 exists systematic anomaly, as the activity elevates significantly in several car parks.

3.6. Spatial-temporal potential exposure risk mapping

Fig. 9 shows the spatial-temporal trend of heat. The four regions, i.e. Bukit Timah, Changi, Downtown Core and Tanglin, have only 2, 2, 1 and 1 residential car parks. As introduced in Section 2.2.1, these four regions should be filtered among the 31 regions in Fig. 4. The resident population in the remaining 27 coloured regions in Fig. 9 covers 96.7% among that of the total of 55 regions in Singapore (DOS, 2019). Overall, the regional heat is reduced significantly after 06 April 2020, especially in these regions with relatively high heat. The significant decreasing trend from 06 April to 12 April 2020 has been observed. The spatial variations are apparent between Sunday and other days. Uncertainties of heat, which manifest as the uncertain fluctuations of heat values (Fig. S4), exist in not only the time horizon but also the space scope. For example, judged by the temporal variation of colours (i.e. heat values) of the regions with high heat in Fig. 9, noticeable fluctuations are observed for the region-level heat on 18 March, 26 March, 03 April, 06 April and 10 April 2020. Due to the uncertainties of heat, it is challenging to yield the spatial exposure risk distribution by simply adopting the distribution of a certain day or aggregating heat values of some days. There is no need to measure the uncertainties quantitatively before the risk mapping modelling, as the Bayesian spatial-temporal risk

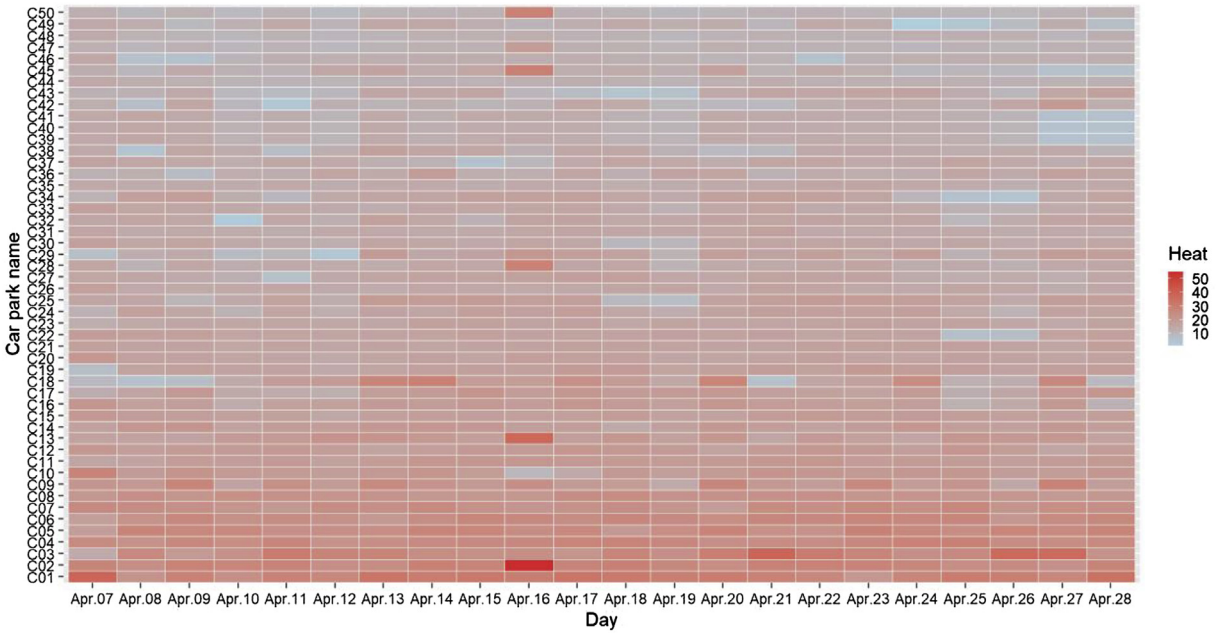

Fig. 8. The temporal heat map of the top 50 most active car parks among residential car parks with the first half of high mobility during the circuit breaker (07 April to 28 April 2020). The car park names numbered as C1 to C50 are anonyms for privacy concerns.

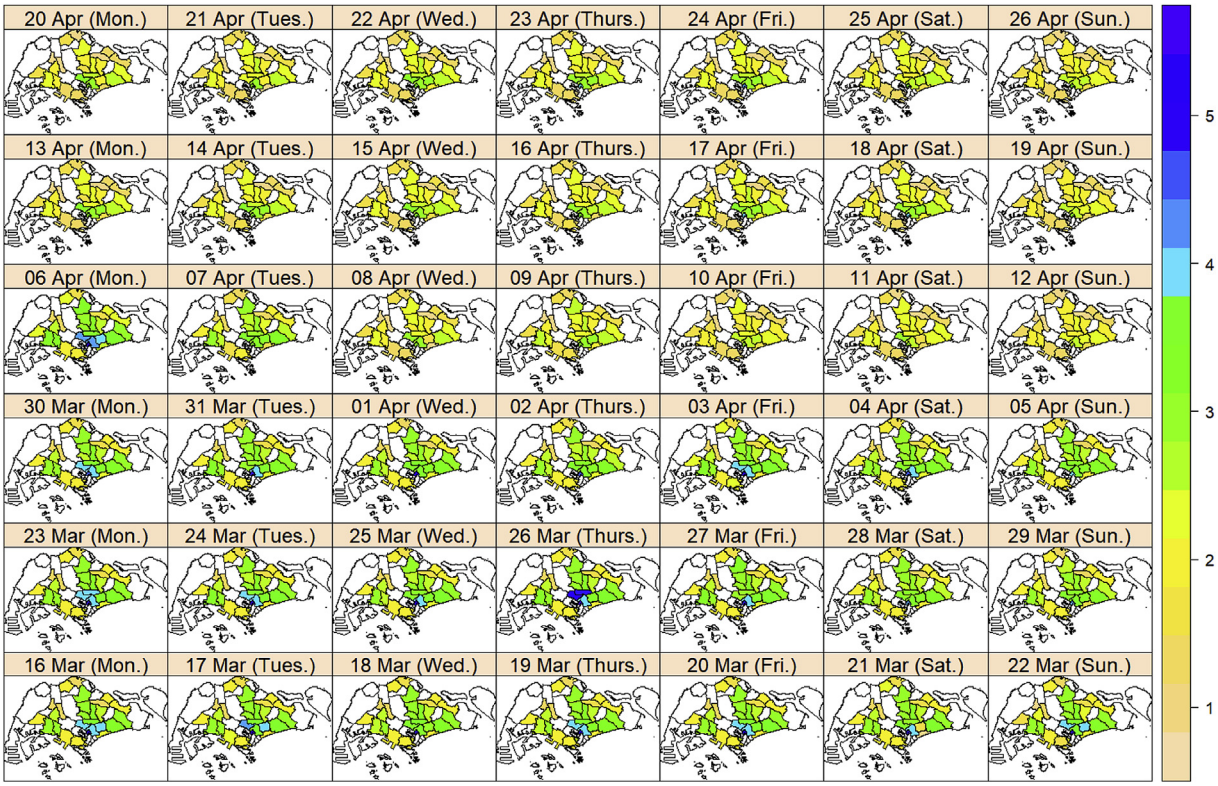

Fig. 9. The spatial-temporal trend of heat from 16 March (Monday) to 26 April (Sunday) 2020. Spatial heat results related to 15 March and 27–28 April are omitted for ease of the weekly presentation.

Table 3
Performance comparison of six spatial-temporal interactions.

Interaction	Type I	Type II*[a]	Type II*[b]	Type III	Type IV*[a]	Type IV*[b]
DIC	13,903	13,893	13,955	13,917	13,912	13,986

Notes: *a denotes the interaction with a first-order random walk; *b denotes the interaction with a second-order random walk.

mapping model in Eqs. (8)–(11) of Section 2.2.4 provides a Poisson regression solution for such a problem with uncertainties of heat.

For the Bayesian spatial-temporal risk mapping modes with different interaction candidates, six spatial-temporal interactions derived from Types I to IV in Eq. (11) are compared to select the best model. Table 3 shows the model selection results based on the minimal deviance information criterion (DIC) (Spiegelhalter et al., 2002), which is introduced in Section 2.2.4. The model with the Type II interaction and a first-order random walk produces the smallest DIC value (i.e. 13,893), which is identified as the best model among the six models.

Based on the best model, Fig. 10 shows the scaled computational results of temporal exposure risks and spatial exposure risks. The temporal exposure risks are the summation of baseline temporal risks and spatial-temporal interacted risks. In Fig. 10a, the calculated risks fit well with the observed heat values. The close match of the curves indicates the adequacy of the spatial-temporal statistical model. Temporal exposure risks are reduced significantly after implementing the circuit breaker policy. The average reduction rate exceeds 30.0% compared to the day before the circuit breaker. Compared to the peak value, the maximal reduction rate of potential exposure risk reaches 37.6%. The spatial exposure risks include intrinsic spatial risks and spatial-temporal interacted risks. Fig. 10b shows the scaled spatial exposure risks for a total of 27 coloured regions. Fig. 10b offers an intuitive impression on the potential exposure risks of individual regions and their relative hazards. Such a visualisation could be helpful for decision-makers, especially when resources are limited to disease mitigation. The areas with top 5 or top 10 exposure risks can be easily identified. As a supplement to decision support, Fig. 10c shows the six-level division results of scaled spatial risks from Fig. 10b.

4. Discussion

4.1. The circuit breaker policy in Singapore

Fig. 5b demonstrated the effectiveness of the circuit breaker in Singapore. Two crucial questions should be of interest for the decision-makers in implementing the circuit breaker policy. First, is the time right for the circuit breaker policy? The sub-exponential or polynomial growth has been observed for other Chinese provinces except for Hubei (Roosa et al., 2020), South Korea (Shim et al., 2020) and Singapore (Tariq, 2020). The exponential growth has been observed for those epicentre areas, including Italy, Spain (Saez et al., 2020) and Hubei province of China (Roosa et al., 2020). In this study, the three-order polynomial trend in Fig. 5b is identified to fit the second-wave disease outbreak well in Singapore. However, during the last several days in Phase I, there has been already an indication of a possibly exponential-growth trend (Fig. 5c). This kind of evidence indicates that the decision on the time of starting the circuit breaker (07 April 2020) is cautious and prescient. Second, when does the turning point of community spread appear? According to the curves in Fig. 5a and 5b, the increasing trend slows down from 22 April 2020. In other words, the turning point appears for the exposure-related cases on the 16th day after implementing the circuit breaker. The trend indicates the disease situation in the community gets stable under the mitigation measures. However, this trend does not guarantee a non-occurrence of a new-wave disease outbreak. This might be the reason why the government authority in Singapore extends the circuit breaker from 05 May to

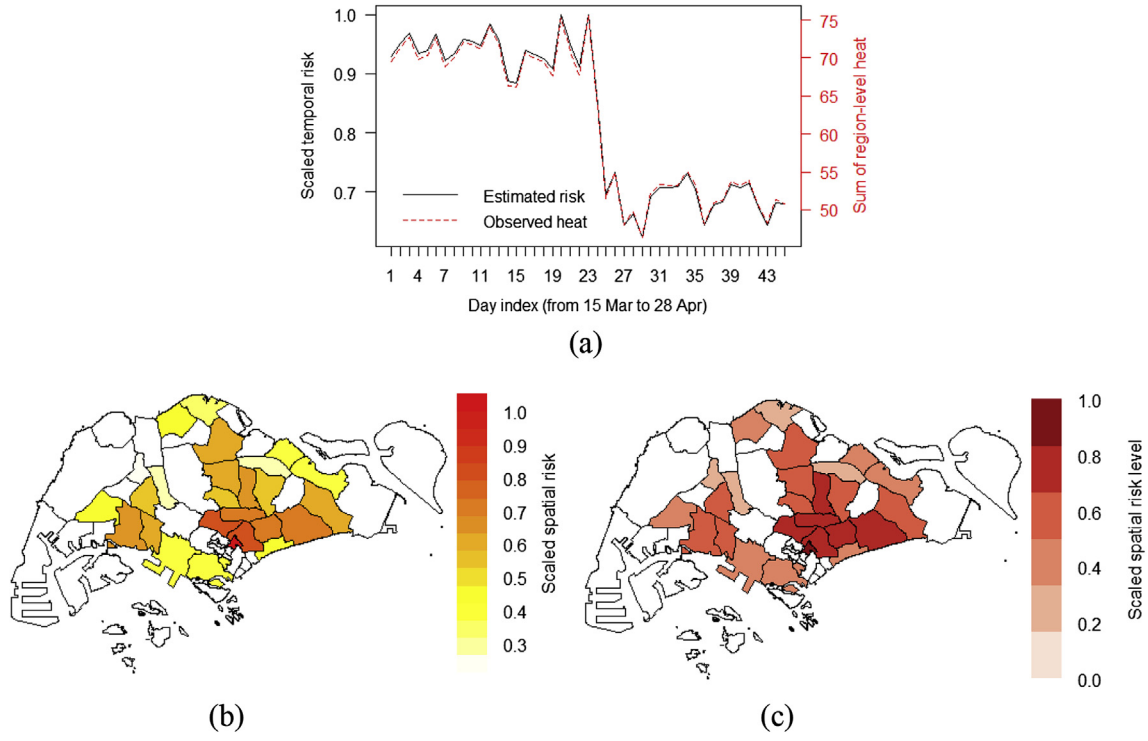

Fig. 10. Visualisation for (a) the scaled temporal exposure risks from 15 March to 28 April 2020, (b) the scaled spatial exposure risks and (c) the six-level division of scaled spatial risks. The temporal risks and spatial risks are scaled based on their respective maximal risk values.

01 June 2020.

4.2. Lockdown/circuit breaker & urban sustainability

The lockdown or circuit breaker policy is a double-edged sword (Gilbert et al., 2020). On the one hand, it reduces the potential exposure risk of infection and further brings nations back to regular status. On the other hand, it changes the economic structure and lifestyle rapidly, which causes more challenges for almost every aspect of urban sustainability, especially in environment health and economy development (Chakraborty and Maity, 2020). Regarding environmental sustainability, although single-use plastics in regular life and medical waste are elevated sharply, the total municipal waste is not necessarily increased. An additional 1,334 t of household plastic waste was estimated to be produced by residents in Singapore during the circuit breaker period in April and May 2020 (Low and Koh, 2020). Few densely populated cities (e.g. Manila, Jakarta, Kuala, Bangkok, Ha Noi and Wuhan) have the capacity to cope with the excessive amounts of medical waste during disease pandemic (Asian Development Bank, 2020). The average solid waste amount in large and medium cities in China was estimated to be reduced by about 30.0% during the COVID-19 outbreak (Liu, 2020). In contrast, the average domestic waste amount in Singapore is elevated by about 3% during the circuit breaker (Low and Koh, 2020). Worldwide air emissions have been significantly reduced during lockdown periods. Evidence can be found from cases in China (Bao and Zhang, 2020) and Brazil (Dantas et al., 2020). The calculation in this study indicates that a) the average electricity consumption during the circuit breaker has a 6.7% reduction in Singapore, and b) the transportation-related average air emissions in Singapore are reduced by 44.3% (Fig. 6a) and 55.4% (Fig. 6b) under two scenarios. Greenhouse gas emissions and air pollutants have to be assessed simultaneously (Fan et al., 2018) across different sectors, not limited to transportation. This is important to prevent the shifting of environmental footprints and for a conclusive picture, as the pandemic could have changed the economic and social structure considerately. Although the lasting impact on environmental sustainability still requires a systematic assessment, economic sustainability is cautiously thought to be the major issue to maintain urban sustainability. During each disease pandemic, public health should be prioritised over all other considerations; meanwhile, economic restart and recovery plans need to be developed suitably (Klemeš et al., 2020b). The worldwide economic sustainability has been severely threatened. Fernandes (2020) estimated that GDP growth ranges from −3.5% to −6% in different countries if the shutdown of economic activity lasts for 1.5 months. Nicola et al. (2020) reviewed the socio-economic impacts of COVID-19 on different sectors, including agriculture, petroleum, manufacturing, education, finance, healthcare, tourism, sports and food. Economic sustainability and its recovery are highly related to lockdown exit strategies, as discussed in Section 4.3.

4.3. Economic sustainability & lockdown exit strategies

As governments cannot minimise both the economic impact of COVID-19 and the deaths caused by COVID-19 (Anderson et al., 2020), the nation managers worldwide have a high probability of facing the trade-offs between risk reduction via extending a circuit breaker and economic recovery by lifting a circuit breaker. At the beginning of May 2020, such a dilemma is haunting worldwide countries, such as the USA, Singapore, India, Spain, Germany and Italy. For a more specific example, the Straits Times has pointed out that the Singapore economy plunges in coronavirus pain, and the quarter-on-quarter growth of the first quarter of 2020 will be −10.6% (Subhani, 2020). On 26 May 2020, Ministry of Trade and Industry (MTI) has slashed its economic growth forecast in 2020 to a range of −7.0% to −4.0% (MTI, 2020b), from the estimate of −4.0% to −1.0% (MTI, 2020a) on 26 March (before the circuit breaker) and the estimate of −0.5% to 1.5% (MTI, 2020a) during the first-wave disease outbreak. Global economic recession due to disease pandemic leads to company bankruptcy and unemployment, which might cause a series of 'butterfly effects' for the whole society, including the adverse effects on disease prevention and control. After implementing more than one-month circuit breaker, the disease surge in the community of Singapore has shown an easing trend (Fig. 5b), without considering the cases of confined areas. What is the next step in the near or far away future? Regarding lockdown exit strategies, other than an overall lockdown exit strategy and the responsible lockdown exit strategy (Gilbert et al., 2020) (e.g. systematic tests, contact tracing and priority rework of people with a low-risk profile), the flexible local circuit breaker strategy and the precise management measures might be beneficial for the whole society. In the following, we extend the discussion and offer several suggestions from the perspective of spatial-temporal potential exposure risks.

4.4. Spatial exposure-risk distribution & flexible local circuit breaker

The report from Harvard University suggested that intermittent or prolonged social distancing might be necessary into 2022 (Kissler et al., 2020). One of the negative cases occurred in Germany, where the infection rate is rising just days after Germany eased the nationwide lockdown (BBC, 2020). Conservatively, a flexible local circuit breaker based on big urban data analytics may be an alternative way of lifting lockdown. The spatial exposure-risk distribution in Fig. 9b and 9c can be used to identify crucial regions with high potential exposure risk for maintaining local circuit breaker. Notably, the region with the highest mobility in Fig. 4 is not necessarily the riskiest region measured by heat in Fig. 8. Those regions with moderate and low potential exposure risks may gradually lift the restriction measures; however, residents should be aware of avoiding high-risk areas. The decision on the range of local circuit breaker can be adjusted dynamically according to the performance of these crucial regions and the overall disease mitigation effects. For crucial regions with high potential exposure risks, e.g. regions with dark red colours in Fig. 10c, strict but flexible measures are also needed, such as 1) the segregation plan with Team-A and Team-B to reduce about half of the working crowds, and 2) working under permission if essential works require to be done.

4.5. Peak hour distribution & temporal crowd division

When relaxing the circuit breaker, the mobility has a high probability back to the regular situation from 15 March to 06 April 2020 (Figs. 3 and 4) unless additional measures are taken. Peak hour distribution of mobility would be enlarged significantly, especially 07:00–08:00 and 18:00–19:00 on working days, as shown in Fig. 3a, 3b and 3c. In the aspect of working, a more flexible working duration is recommended for staffs to decrease the peaks. Effective regulations on working hours can be coordinated among firms according to real-time monitoring and peak hour analytics. In the aspect of life at home, residents can acquire more online information on the distribution of crowds, as shown in Fig. 3e and 3f, and select a suitable time to go outside buying necessities to avoid peak hours and crowds. Government authority may regulate the extension of working hours of shops to divert the crowd. The above measures can promote an effective temporal crowd division based on the information of peak hour distribution.

4.6. Mobility heat map & key hotspot identification

Worldwide experiences have demonstrated the effects of social distancing and circuit breaker in mitigating infectious diseases, e.g. COVID-19 (Saez et al., 2020). To ensure the effectiveness of ongoing policies and not to waste the efforts of other residents, the government authority may pay more attention to those residential areas with both high mobility and high heat. This study makes such precise management possible via tracing the mobility heat map. As shown in Figs. 7 and 8, the hotspots of mobility can be quickly identified. The hotspot identification allows zooming to specific locations for precise mitigation based on the evidence of the calculated mobility index in Fig. 7. Then, a) appropriate warning or punishment against uncooperative/illegal acts of the hotspot communities and b) timely anonymous notification via social media may consolidate the circuit breaker management efficiently.

4.7. Phase-related dynamic curve fitting & timely decision-making

The exponential trend can only fit the confirmed cases in the early stage of the COVID-19 outbreak (Remuzzi and Remuzzi, 2020). It is complicated to estimate the trend in a country with ongoing disease outbreak via other countries' experiences due to the differences in social distancing measures and facility capacity (Remuzzi and Remuzzi, 2020). What makes the problem challenging is that the social distancing measures would change in different mitigation phases in the same country. This study innovatively separates the time duration of pandemic mitigation and the time series of confirmed cases into different phases according to the adjusted measures in Singapore. Under different phases, the curves in Fig. 5b with the best-identified lag period (Table 2) fit well between the cumulative lagged mobility and the exposure-related cases in Singapore. In a specific phase, the dynamic curve fitting, as illustrated in Fig. 5c, offers a visual impression on the variation of the fitted trend. This phase-related dynamic curve fitting method can be used further to separate the time in subsequent mitigation period. Timely decisions are suggested being made based on the trend of the dynamically updated curve fitting.

It has been already a suitable time to look forward to the post-pandemic period, and it has to be maintained a foresight perspective for the future. For example, what has been seen in Europe, the population is still uneasy about using public transport and is predominantly moving to cars. Such social consciousness is being cultivated by the COVID-19 epidemic and even more by the pandemic. What has been a high probability is that urban sustainability could be influenced profoundly, and air emissions might increase worldwide compared to the regular time before COVID-19 pandemic. During and after the disease outbreak, timely decision-making and consciousness training deserve more attention and especially planning, even if it may be needed using some likely scenarios as, e.g. the second and following waves.

4.8. Limitation and strength

Each study has some limitations naturally. First, the car mobility of this study is approximated by the dynamically updated data on available lots of car parks. However, Biljecki (2020) suggested that car park availability data can be regarded as a good proxy for the movement of people in the absence of better data. The results and applicability of the method proposed in this study are still valid despite the limitation. This is the case, especially when the change in car mobility behaviour is a relative concept.

Second, although the driving mobility has been observed as a good representation of population mobility in terms of walking, driving and transit (Fig. S1), macro population mobility is just a component of the entire daily mobilities in society. The higher heat at some specific car parks and even at some specific regions cannot totally represent micro human interactions. The other micro factors, such as the destination (e.g. crowded) and the person who has met with, are having a considerate impact on the infection risk. However, it is an open and challenging task to measure the entire daily mobilities at both macro and micro levels. It needs to integrate more subsystems for such a task, as stated in the future work agenda.

The strength of the proposed method is that there is a massive high-resolution spatial-temporal data with usually every-minute updating available for big urban data analytics and modelling before and during the circuit breaker. Buckee et al. (2020) appealed to the society that aggregated mobility data with real-time information have been urgently needed to fight the COVID-19 pandemic. This study provides a novel perspective and puts a small step forward on this topic.

5. Conclusions

This study has provided a novel perspective to analyse the spatial-temporal potential exposure risk of COVID-19 by capturing human behaviours based on high-resolution data of car park availability. A testing ground, Singapore, which is threatened by a second coronavirus wave from the beginning of April 2020, has illustrated the analytical procedure and demonstrated its applicability. For a nation or an area with available spatial-temporal data on mobility, the proposed method offers a possibility for precise urban management (i.e. the hotspot identification and temporal crowd division) and timely decision-making related to COVID-19 mitigation. Regarding urban sustainability, although there is an apparent improvement in environmental performance, arises from the lockdown measures, e.g. the pollution reduction by transportation and industrial sector, the long-term impact of environmental sustainability requires to be assessed further. The post effect, especially dealing with medical waste disposal and single-use plastics should also be considered. When the epidemic/pandemic eases during the lockdown or circuit breaker period, the main challenges lie in economic sustainability and its recovery, as the mitigation measure makes many social contacts and production activities pause citywide. The spatial-temporal potential exposure risk analytics in this study offers intelligent decision support to plan a flexible local circuit breaker strategy, by which the decision-makers might be guided to gradually reopen partial regions of the city or country for economic recovery.

5.1. Quantitative results

The quantitative results derived from the Singapore case, being obviously of crucial importance, are summarised as follows:

a) The reduction rate of mobility reaches 36.4% in the first week during the circuit breaker. It maintains at around 30.0% in the following two weeks. Compared to regular times, the morning peaks on working days during the circuit breaker almost disappear, which are dominated slightly by the noon peaks.
b) Three-order polynomial (i.e. sub-exponential) functions well fit the curves between cumulative lagged mobility and cumulative cases (exposure-related cases) for both two phases. The six-day lag setting produces the smallest sum of squared residuals than other lag settings.
c) The 16th day after implementing the circuit breaker policy is observed as the turning point for the exposure-related

COVID-19 cases, by which the cumulative exposure-related cases tend to present a gradually decreasing trend.

d) The longtail characteristic is observed for the probability distributions of both nationwide mobility (skewness = 0.99) and nationwide heat (skewness = 3.86), indicating that, regarding the hotspot identification, decision-makers should focus on the intersection of both longtail parts, rather than those active car parks with high heat only.

e) The transportation-related average air emissions are estimated to be reduced by 44.3% (Scenario 1) to 55.4% (Scenario 2) during the circuit breaker, indicating that the circuit breaker not only keeps residents safe but also contributes to environmental health from the transportation pollution perspective. This would be more interesting by simultaneously considering that the disease pandemic triggers some companies, e.g. Twitter, to let some employees work from home 'forever' if they choose (Fung, 2020).

f) The average daily electricity consumption during the circuit breaker is reduced by 6.7% compared to that before the circuit breaker. The 2020 economic growth forecast in Singapore has been slashed to a range of −7.0% to −4.0% (MTI, 2020b).

g) The maximal reduction rate of potential exposure risk reaches 37.6% by comparing with its peak value. Fluctuations and uncertainties along the time horizon have been observed for the heat and potential exposure risks, implying the spatial-temporal interactions among different regions.

5.2. Future work

At least two research directions deserve investigations in future.

(i) It is worthwhile to integrate more subsystems under big urban data, e.g. transportation, environment, electricity, express delivery and social media, into a comprehensive platform to guide decision-making better in a system-of-systems manner under the premise of privacy protection.

(ii) Since the exposure risk defined in this study has a 'relative' and 'potential' concept, there is not necessarily a strong causality between spatial potential exposure risks and regional infection rates. While the possible relationship between them still deserves to be investigated with regional infection data available in future.

Disclaimer

The views expressed are those of the authors and do not necessarily represent the official policy of the Agency for Science, Technology and Research (A*STAR) and the Ministry of Health (MOH) in Singapore.

CRediT authorship contribution statement

Peng Jiang: Conceptualization, Data curation, Methodology, Formal analysis, Visualization, Writing - original draft. **Xiuju Fu:** Conceptualization, Methodology, Writing - review & editing, Validation, Funding acquisition. **Yee Van Fan:** Conceptualization, Methodology, Writing - original draft. **Jiří Jaromír Klemeš:** Conceptualization, Methodology, Writing - review & editing, Funding acquisition. **Piao Chen:** Methodology, Writing - review & editing. **Stefan Ma:** Writing - review & editing, Validation. **Wanbing Zhang:** Data curation.

Declaration of competing interest

The authors declare that they have no known competing financial interests or personal relationships that could have appeared to influence the work reported in this paper.

Acknowledgements

This work was partially supported by the National Research Foundation Singapore under grant No. NRF2017VSG-AT3DCM001-045. The financial support from the EU supported project Sustainable Process Integration Laboratory – SPIL funded as project No. CZ.02.1.01/0.0/0.0/15_003/0000456, by Czech Republic Operational Programme Research and Development, Education, Priority 1: Strengthening capacity for quality research is acknowledged.

Appendix A. Supplementary data

Supplementary data to this article can be found online at https://doi.org/10.1016/j.jclepro.2020.123673.

References

Anderson, R.M., Heesterbeek, H., Klinkenberg, D., Hollingsworth, T.D., 2020. How will country-based mitigation measures influence the course of the COVID-19 epidemic? Lancet 395 (10228), 931–934.

Apple, 2020. Mobility Trends Reports. Accessed 20.05.2020. https://www.apple.com/covid19/mobility.

Asian Development Bank, 2020. Managing infectious medical waste during the COVID-19 pandemic. Accessed 06.07.2020. https://www.adb.org/sites/default/files/publication/578771/managing-medical-waste-covid19.pdf.

Bao, R., Zhang, A., 2020. Does lockdown reduce air pollution? Evidence from 44 cities in northern China. Sci. Total Environ. 731, 139052.

BBC, 2020. Coronavirus: Germany infection rate rises as lockdown eases. Accessed 20.05.2020. https://www.bbc.com/news/world-europe-52604676.

Biljecki, F., 2020. Singapore's urban data affirms the compliance with the Circuit Breaker measures. Accessed 20.05.2020. https://ual.sg/post/2020/04/12/singapores-urban-data-affirms-the-compliance-with-the-circuit-breaker-measures/.

Blangiardo, M., Cameletti, M., 2015. Spatial and Spatio-Temporal Bayesian Models with R-INLA. John Wiley & Sons, Chichester, West Sussex, UK.

Buckee, C.O., Balsari, S., Chan, J., Crosas, M., Dominici, F., Gasser, U., Grad, Y.H., Grenfell, B., Elizabeth Halloran, M., Kraemer, M.U.G., Lipsitch, M., Metcalf, C.J.E., Meyers, L.A., Alex Perkins, T., Santillana, M., Scarpino, S.V., Viboud, C., Wesolowski, A., Schroeder, A., 2020. Aggregated mobility data could help fight COVID-19. Science 368 (6487), 145–146.

CE Delft, 2020. STREAM passenger transport. Accessed 20.05.2020. https://www.cedelft.eu/en/stream-passenger-transport.

Chakraborty, I., Maity, P., 2020. COVID-19 outbreak: migration, effects on society, global environment and prevention. Sci. Total Environ. 728, 138882.

Collivignarelli, M.C., Abbà, A., Bertanza, G., Pedrazzani, R., Ricciardi, P., Miino, M.C., 2020. Lockdown for CoViD-2019 in Milan: what are the effects on air quality? Sci. Total Environ. 732, 139280.

Cressie, N., Wikle, C.K., 2015. Statistics for Spatio-Temporal Data. John Wiley & Sons, US.

CSD, 2020. Motor vehicle population by type of fuel used. Customer Services Division (CSD). https://www.lta.gov.sg/content/dam/ltagov/who_we_are/statistics_and_publications/statistics/pdf/M09-Vehs_by_Fuel_Type.pdf. Accessed 20.05.2020.

Cyranoski, D., 2020. 'We need to be alert': scientists fear second coronavirus wave as China's lockdowns ease. Nature News. https://www.nature.com/articles/d41586-020-00938-0. Accessed 20.05.2020.

Dantas, G., Siciliano, B., França, B.B., da Silva, C.M., Arbilla, G., 2020. The impact of COVID-19 partial lockdown on the air quality of the city of Rio de Janeiro, Brazil. Sci. Total Environ. 729, 139085.

DBS, 2020. Reinventing the wheel: the future of automotive. https://www.dbs.com.sg/iwov-resources/forms/sgsme/en/businessclass/events/disrupt-at-the-bay/automotive-report.pdf. Accessed 20.05.2020.

Diao, M., 2019. Towards sustainable urban transport in Singapore: policy instruments and mobility trends. Transport Pol. 81, 320–330.

DOS, 2019. Population Trends 2019. Department of Statistics (DOS). https://www.singstat.gov.sg/-/media/files/publications/population/population 2019.pdf. Accessed 20.05.2020.

EMA, 2020. Historical electricity system demand for every half hour period (MW). Energy Market Authority (EMA), Singapore. https://www.ema.gov.sg/statistic.aspx?sta_sid=20140826Y84sgBebjwKV. Accessed 20.05.2020.

Fan, Y.V., Perry, S., Klemeš, J.J., Lee, C.T., 2018. A review on air emissions assessment: Transportation. J. Clean. Prod. 194, 673–684.

Fan, Y.V., Klemeš, J.J., Walmsley, T.G., Perry, S., 2019. Minimising energy consumption and environmental burden of freight transport using a novel graphical decision-making tool. Renew. Sustain. Energy Rev. 114, 109335.
Ferguson, N.M., Laydon, D., Nedjati-Gilani, G., Imai, N., Ainslie, K., Baguelin, M., et al., 2020. Impact of Non-pharmaceutical Interventions (NPIs) to Reduce COVID-19 Mortality and Healthcare Demand. COVID-19 Reports. Faculty of Medicine, Imperial College, London, UK. https://doi.org/10.25561/77482, 2020.
Fernandes, N., 2020. Economic effects of coronavirus outbreak (COVID-19) on the world economy. Available at SSRN: https://doi.org/10.2139/ssrn.3557504.
Fogarty, D., 2020. Air Pollution Clears in Some Cities in South-East Asia during Lockdowns, but Not All, Study Finds. The Straits Times. https://www.straitstimes.com/asia/se-asia/air-pollution-clears-in-some-cities-in-se-asia-during-lockdowns-but-not-all-study-finds. Accessed 20.05.2020.
Fung, B., 2020. Twitter Will Let Some Employees Work from Home 'forever'. CNN Business. https://edition.cnn.com/2020/05/12/tech/twitter-work-from-home-forever/index.html. Accessed 20.05.2020.
Ghosh, I., 2020. Global shutdown: visualising commuter activity in the world's cities. https://www.visualcapitalist.com/covid-19-cities-commuter-activity/. Accessed 20.05.2020.
Gibney, E., 2020. Whose coronavirus strategy worked best? Scientists hunt most effective policies. Nature 581 (7806), 15–16. https://doi.org/10.1038/d41586-020-01248-1.
Gilbert, M., Dewatripont, M., Muraille, E., Platteau, J.P., Goldman, M., 2020. Preparing for a responsible lockdown exit strategy. Nat. Med. 26, 643–644. https://doi.org/10.1038/s41591-020-0871-y.
Giordano, G., Blanchini, F., Bruno, R., Colaneri, P., Di Filippo, A., Di Matteo, A., Colaneri, M., 2020. Modelling the COVID-19 epidemic and implementation of population-wide interventions in Italy. Nat. Med. 26, 855–860. https://doi.org/10.1038/s41591-020-0883-7.
GOS, 2020. What You Can and Cannot Do during the Circuit Breaker Period. Government of Singapore (GOS). https://www.gov.sg/article/what-you-can-and-cannot-do-during-the-circuit-breaker-period. Accessed 20.05.2020.
GTA, 2020a. HDB Carpark Information. Government Technology Agency (GTA). https://data.gov.sg/dataset/hdb-carpark-information?resource_id=139a3035-e624-4f56-b63f-89ae28d4ae4c. Accessed 20.05.2020.
GTA, 2020b. Carpark availability. Government Technology Agency (GTA). https://data.gov.sg/dataset/carpark-availability?resource_id=4f4a57d1-e904-4326-b83e-dae99358edf9. Accessed 20.05.2020.
He, K., Stolarski, A., Whang, E., Kristo, G., 2020. Addressing general surgery residents' concerns in the early phase of the COVID-19 pandemic. J. Surg. Educ. 77 (4), 735–738. https://doi.org/10.1016/j.jsurg.2020.04.003.
Huang, Y., Zhou, B., Li, N., Li, Y., Han, R., Qi, J., Lu, X., Li, S., Feng, C., Liang, S., 2019. Spatial-temporal analysis of selected industrial aquatic heavy metal pollution in China. J. Clean. Prod. 238, 117944.
Jia, J.S., Lu, X., Yuan, Y., Xu, G., Jia, J., Christakis, N.A., 2020. Population flow drives spatio-temporal distribution of COVID-19 in China. Nature 582, 389–394. https://doi.org/10.1038/s41586-020-2284-y.
Jiang, P., Fan, Y.V., Zhou, J., Zheng, M., Liu, X., Klemeš, J.J., 2020. Data-driven analytical framework for waste-dumping behaviour analysis to facilitate policy regulations. Waste Manag. 103, 285–295.
Kissler, S.M., Tedijanto, C., Goldstein, E., Grad, Y.H., Lipsitch, M., 2020. Projecting the transmission dynamics of SARS-CoV-2 through the postpandemic period. Science 368 (6493), 860–868. https://doi.org/10.1126/science.abb5793.
Klemeš, J.J., Fan, Y.V., Jiang, P., 2020a. Plastics: friends or foes? The circularity and plastic waste footprint. Energy Sources, Part A Recovery, Util. Environ. Eff. https://doi.org/10.1080/15567036.2020.1801906.
Klemeš, J.J., Fan, Y.V., Tan, R.R., Jiang, P., 2020b. Minimising the present and future plastic waste, energy and environmental footprints related to COVID-19. Renew. Sustain. Energy Rev. 127, 109883.
Kucharski, A.J., Russell, T.W., Diamond, C., Liu, Y., Edmunds, J., Funk, S., Eggo, R.M., 2020. Early dynamics of transmission and control of COVID-19: a mathematical modelling study. Lancet Infect. Dis. 20 (5), 553–558.
Lai, S., Ruktanonchai, N.W., Zhou, L., Prosper, O., Luo, W., Floyd, J.R., Wesolowski, A., Santillana, M., Zhang, C., Du, X., Yu, H., Tatem, A.J., 2020. Effect of non-pharmaceutical interventions to contain COVID-19 in China. Nature. https://doi.org/10.1038/s41586-020-2293-x.
Lauer, S.A., Grantz, K.H., Bi, Q., Jones, F.K., Zheng, Q., Meredith, H.R., Azman, A.S., Reich, N.G., Lessler, J., 2020. The incubation period of coronavirus disease 2019 (COVID-19) from publicly reported confirmed cases: estimation and application. Ann. Intern. Med. https://doi.org/10.7326/M20-0504.
Li, Q., Guan, X., Wu, P., Wang, X., Zhou, L., Tong, Y., et al., 2020. Early transmission dynamics in Wuhan, China, of novel coronavirus–infected pneumonia. N. Engl. J. Med. 382 (13), 1199–1207. https://doi.org/10.1056/NEJMoa2001316.
Lindgren, F., Rue, H., 2015. Bayesian spatial modelling with R-INLA. J. Stat. Software 63 (19), 1–25.
Liu, L., 2020. Press Conference of the Joint Prevention and Control Mechanism of the State Council, 2020. www.gov.cn/xinwen/gwylflkjz53/index.htm. accessed 20.05.2020.
Low, D.W., Koh, A., 2020. Singapore's Food Delivery Surge during Lockdown Highlights Waste Problems. https://www.bloomberg.com/news/articles/2020-06-24/singapore-binges-on-plastics-ordering-food-during-virus-lockdown. Accessed 07.07.2020.
Luo, J.M., Vu, H.Q., Li, G., Law, R., 2019. Tourist behaviour analysis in gaming destinations based on venue check-in data. J. Trav. Tourism Market. 36 (1), 107–118.
MOH, 2020. Updates on COVID-19 (Coronavirus Disease 2019) Local Situation. Ministry of Health (MOH). https://www.moh.gov.sg/covid-19. Accessed 20.05.2020.
MTI, 2020a. Singapore's GDP Contracted by 2.2 Per Cent in the First Quarter of 2020. MTI Downgrades 2020 GDP Growth Forecast to "−4.0 to −1.0 Per Cent". Ministry of Trade and Industry (MTI). https://www.mti.gov.sg/Newsroom/Press-Releases/2020/03/Singapore-GDP-Contracted-by-2_2-Per-Cent-in-the-First-Quarter-of-2020. Accessed 20.05.2020.
MTI, 2020b. MTI Downgrades 2020 GDP Growth Forecast to "−7.0 to −4.0 Per Cent". Ministry of Trade and Industry (MTI). https://www.mti.gov.sg/Newsroom/Press-Releases/2020/05/MTI-Downgrades-2020-GDP-Growth-Forecast-to–7_0-to–4_0-Per-Cent. Accessed 07.07.2020.
NCIRD, 2020. Public health recommendations for community-related exposure. National Center for Immunization and Respiratory Diseases (NCIRD). https://www.cdc.gov/coronavirus/2019-ncov/php/public-health-recommendations.html. Accessed 20.05.2020.
Nesoff, E.D., Milam, A.J., Pollack, K.M., Curriero, F.C., Bowie, J.V., Knowlton, A.R., Gielen, A.C., Furr-Holden, D.M., 2019. Neighbourhood alcohol environment and injury risk: a spatial analysis of pedestrian injury in Baltimore City. Inj. Prev. 25 (5), 350–356.
Nicola, M., Alsafi, Z., Sohrabi, C., Kerwan, A., Al-Jabir, A., Iosifidis, C., Agha, M., Agha, R., 2020. The socio-economic implications of the coronavirus and COVID-19 pandemic: a review. Int. J. Surg. 78, 185–193.
Numbeo, 2020. Traffic in Singapore. https://www.numbeo.com/traffic/in/Singapore. Accessed 20.05.2020.
Okunlola, O.A., Oyeyemi, O.T., 2019. Spatio-temporal analysis of association between incidence of malaria and environmental predictors of malaria transmission in Nigeria. Sci. Rep. 9 (1), 1–11.
Pung, R., Chiew, C.J., Young, B.E., Chin, S., Chen, M.I.C., Clapham, H.E., et al., 2020. Investigation of three clusters of COVID-19 in Singapore: implications for surveillance and response measures. Lancet 395 (10229), 1039–1046. https://doi.org/10.1016/S0140-6736(20)30528-6.
Queiroz, N., Humphries, N.E., Couto, A., Vedor, M., da Costa, I., Sequeira, A.M.M., et al., 2019. Global spatial risk assessment of sharks under the footprint of fisheries. Nature 572 (7770), 461–466.
Remuzzi, A., Remuzzi, G., 2020. COVID-19 and Italy: what next? Lancet 395 (10231), 1225–1228.
Roosa, K., Lee, Y., Luo, R., Kirpich, A., Rothenberg, R., Hyman, J.M., Yan, P., Chowella, G., 2020. Real-time forecasts of the COVID-19 epidemic in China from february 5th to february 24th, 2020. Infectious Disease Modelling 5, 256–263.
Rue, H., Martino, S., Chopin, N., 2009. Approximate Bayesian inference for latent Gaussian models by using integrated nested Laplace approximations. J. Roy. Stat. Soc. B 71 (2), 319–392.
Rumson, A.G., Hallett, S.H., 2019. Innovations in the use of data facilitating insurance as a resilience mechanism for coastal flood risk. Sci. Total Environ. 661, 598–612.
Saez, M., Tobias, A., Varga, D., Barceló, M.A., 2020. Effectiveness of the measures to flatten the epidemic curve of COVID-19. The case of Spain. Sci. Total Environ. 727, 138761.
SGTrafficWatch, 2020. Realtime Singapore traffic watch. https://sgtrafficwatch.org/. Accessed 20.05.2020.
Shim, E., Tariq, A., Choi, W., Lee, Y., Chowell, G., 2020. Transmission potential and severity of COVID-19 in South Korea. Int. J. Infect. Dis. 93, 339–344.
Sikder, S.K., Behnisch, M., Herold, H., Koetter, T., 2019. Geospatial analysis of building structures in megacity Dhaka: the use of spatial statistics for promoting data-driven decision-making. Journal of Geovisualization and Spatial Analysis 3 (1), 7.
Spiegelhalter, D.J., Best, N.G., Carlin, B.P., Van Der Linde, A., 2002. Bayesian measures of model complexity and fit. J. Roy. Stat. Soc. B 64, 583–639.
Subhani, O., 2020. Singapore economy could be headed for its worst-ever contraction this year. The Straits Times. https://www.straitstimes.com/business/economy/singapore-economy-shrinks-22-in-q1-full-year-growth-forecast-slashed-to-4-to-1. Accessed 20.05.2020.
Sun, L., Axhausen, K.W., 2016. Understanding urban mobility patterns with a probabilistic tensor factorisation framework. Transp. Res. Part B Methodol. 91, 511–524.
Tariq, A., Lee, Y., Roosa, K., Blumberg, S., Yan, P., Ma, S., Chowell, G., 2020. Real-time monitoring the transmission potential of COVID-19 in Singapore, March 2020. BMC Med. 18, 1–14.
Unacast, 2020. Covid-19 social distancing scoreboard – unacast. https://www.unacast.com/covid19/social-distancing-scoreboard. Accessed 20.05.2020.
UNenvironmnet, 2020. Record global carbon dioxide concentrations despite COVID-19 crisis. https://www.unenvironment.org/news-and-stories/story/record-global-carbon-dioxide-concentrations-despite-covid-19-crisis. Accessed 20.05.2020.
Van Bavel, J.J., Baicker, K., Boggio, P., Capraro, V., Cichocka, A., Cikara, M., et al., 2020. Using social and behavioural science to support COVID-19 pandemic response. Nature Human Behavior. https://doi.org/10.1038/s41562-020-0884-z.
Walensky, R.P., del Rio, C., 2020. From mitigation to containment of the COVID-19 pandemic: putting the SARS-CoV-2 genie back in the bottle. J. Am. Med. Assoc. 323 (19), 1889–1890. https://doi.org/10.1001/jama.2020.6572.
Wang, C.J., Ng, C.Y., Brook, R.H., 2020. Response to COVID-19 in Taiwan: big data analytics, new technology, and proactive testing. J. Am. Med. Assoc. 323 (14), 1341–1342.
WHO, 2020. Coronavirus Disease (COVID-2019) Situation Reports. World Health Organization (WHO). https://www.who.int/emergencies/diseases/novel-

coronavirus-2019/situation-reports. Accessed 20.05.2020.
Wu, S., Zhou, S., Bao, H., Chen, D., Wang, C., Li, B., Tong, G., Yuan, Y., Xu, B., 2019. Improving risk management by using the spatial interaction relationship of heavy metals and PAHs in urban soil. J. Hazard Mater. 364, 108–116.
Xu, M., Zhu, S., Zhang, Y., Wang, H., Fan, B., 2019. Spatial-temporal economic analysis of modern sustainable sanitation in rural China: resource-oriented system. J. Clean. Prod. 233, 340–347.
Zhang, T., Fu, X., Ma, S., Xiao, G., Wong, L., Kwoh, C.K., Lees, M., Lee, G.K.K., Hung, T., 2012. Evaluating temporal factors in combined interventions of workforce shift and school closure for mitigating the spread of influenza. PloS One 7 (3), e32203.
Zhang, Y., Wang, X., Li, Y., Ma, J., 2019. Spatiotemporal analysis of influenza in China, 2005–2018. Sci. Rep. 9 (1), 1–12.
Zhao, M., Sun, Z., Zeng, Y., 2020. Exploring urban risk reduction strategy based on spatial statistics and scenario planning. J. Clean. Prod. 264, 121668.